Cloud Radiative Heating Rate Forcing Using Profiles of Retrieved Arctic Cloud Microphysics

M. D. Shupe
Science and Technology Corporation
National Oceanic and Atmospheric Administration
Environmental Technology Laboratory
Boulder, Colorado

P. Zuidema
National Research Council
National Oceanic and Atmospheric Administration
Environmental Technology Laboratory
Boulder, Colorado

T. Uttal
National Oceanic and Atmospheric Administration
Environmental Technology Laboratory
Boulder, Colorado

Introduction

Clouds and their radiative impacts are of primary importance to the Arctic climate and, therefore, global climate. Clouds dominate the radiation balance within the cold, dry Arctic atmosphere, and cloud-radiation feedbacks are closely linked with the snow/ice-albedo feedback. Despite the importance of clouds in the Arctic, our current understanding of these clouds remains limited. Global climate models poorly predict fundamental quantities such as total cloudiness and surface temperature in the Arctic (Chen et al. 1995; Tao et al. 1996), which casts doubt on their ability to predict accurate radiation fields. Cloud observations with potential for improving Arctic models, have historically been restricted by the long Polar night, frequently occurring temperature inversions, and the highly reflective Arctic surface.

In 1997-1998, a large multi-agency effort made the Surface Heat Budget of the Arctic Ocean (SHEBA) Program possible (Uttal et al. 2002). During the field portion of this program, an ice camp moved with the ice pack in the Beaufort and Chukchi Seas for one year. Surface-based remote sensors generated an invaluable new dataset on Arctic cloud properties. The presence of a cloud radar and the application of Arctic-specific retrievals resulted in a yearlong cloud microphysical dataset for SHEBA (Shupe et al. 2001). This data allows for observationally based calculations of radiative heating rate profiles within the Arctic atmosphere.

In this paper we define cloud radiative heating rate forcing (CRHF) as the difference between the all-sky and the clear-sky heating rates. This definition is analogous to the top-of-the-atmosphere and/or surface cloud radiative forcing term presented by Ramanathan et al. (1989), and makes explicit the vertically

resolved contribution of clouds to atmospheric radiative heating rates. From this forcing perspective we present the results of two case studies: one all-ice and one mixed-phase. In the first, three sensitivity studies examine: (1) the difference in heating rates caused by the use of profiles of ice particle size, layer-mean particle size, and fixed particle size; (2) the impact of cloud ice water path (IWP) variability/ uncertainty on the radiative heating profile; and (3) the dependence on solar zenith angle (SZA) (and thereby on location and time of year). In the second, mixed-phase, case we examine the sensitivity of heating rate profiles to the vertical distribution of liquid within the cloud. Mixed-phase clouds are ubiquitous in the Arctic atmosphere, accounting for nearly half of the clouds observed during April-July 1998 (Shupe et al. 2001). They are also the most difficult to characterize using current surface-based remote sensing instrumentation and techniques.

Measurements

To calculate radiative heating rates we use a number of input data streams from SHEBA. A summary of the radar-based techniques used for cloud microphysical retrievals is presented in Shupe et al. (2001). These techniques retrieve vertically resolved profiles of cloud water content and particle size for both liquid and ice clouds from radar and radiometer measurements. Temperature and moisture profiles are obtained from twice-daily soundings and interpolated to the 10-minute time scale used for radiation calculations. The surface albedo is prescribed by spectrally resolved measurements made from a 200 m albedo line near the SHEBA ice camp. Measurements made at the Atmospheric Radiation Measurement (ARM) - North Slope of Alaska (NSA) site are nearly identical to those made at SHEBA, allowing for similar radiative transfer calculations to be made at that location.

Radiative Transfer Model Description

Atmospheric radiative heating rates are calculated using the Streamer radiative transfer (RT) algorithm (Key 2001). This package is widely used in the Arctic research community. Streamer has 24 shortwave (SW) and 105 longwave (LW) bands. We utilize its two-stream solver for calculating fluxes and heating rates. The SW optical property parameterizations for seven different ice particle shapes, including aggregates, are available (Key et al. 2002). The LW ice cloud optical property parameterizations are based on Mie calculations using spherical particles. For these calculations, a standard ozone profile was used as well as the Arctic haze profile that is built into Streamer.

All-Ice Case - April 28, 1998

On April 28, 1998, a single-layer all-ice cloud advected over the SHEBA cloud radar. For this case, a retrieval using both the cloud radar and infrared measurements from the Atmospheric Emitted Radiance Interferometer (AERI) was performed (Matrosov 1999). The mean retrieved ice water content (IWC) on this day is 0.0044 g m^{-3} and the mean ice particle effective radius is 88 μm. Figure 1a shows the 0.6 μm volume extinction coefficient field for this case as calculated by Streamer. The SZA ranged from 86° at 1400 Universal Time Coordinates (UTC) to 62° at 2245 UTC (solar noon). The snow-covered surface
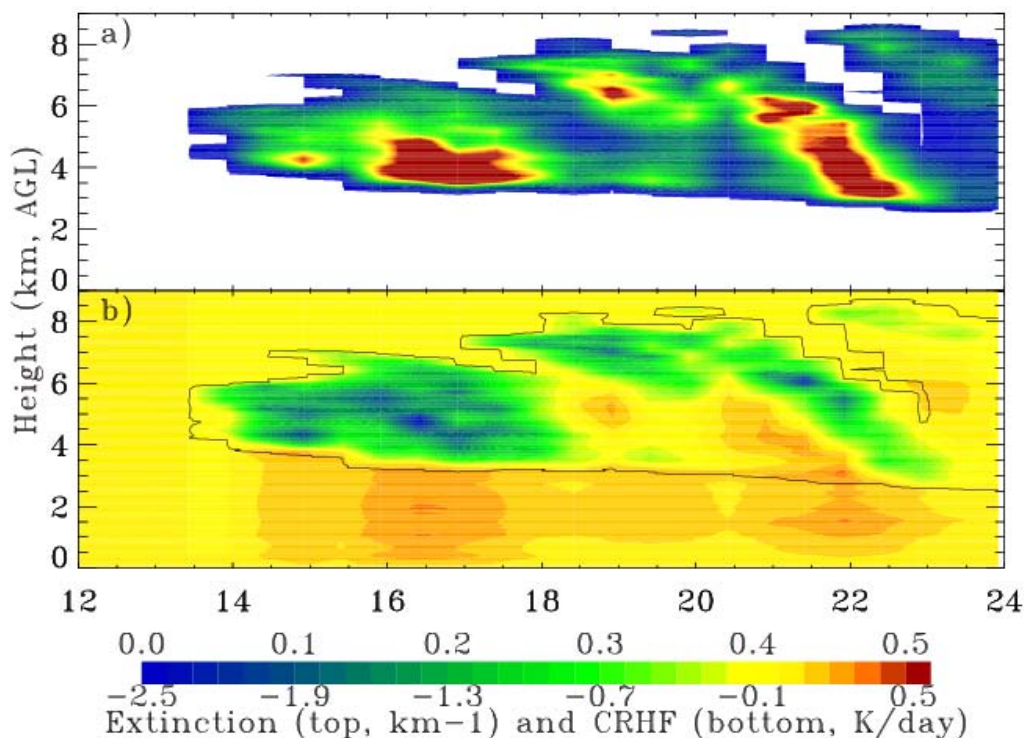
Figure 1. Time-height fields of (a) 0.6 μm volume extinction coefficient and (b) cloud radiative heating rate forcing on April 28, 1998, at SHEBA.

had a mean broadband surface albedo of 0.85. Radiative cloud forcing at the surface was a net warming with a peak in the warming of 35 W m^{-2}. The surface forcing was dominated by LW warming and modulated by SW cooling, which peaked at solar noon.

The time-height cross section of CRHF for this case is shown in Figure 1b. This geometrically thick but optically thin cirrus layer predominantly shows net radiative cooling throughout most of the cloud, with some cells of net radiative heating (e.g., ~1800-2200 from ~4-6 km). The heating cells are optically thin regions that are being radiatively shielded from space by optically thicker cloud regions occurring above them. It is also interesting to note the warming effect this cloud has on the atmosphere below the cloud. The warming results because the cloud more effectively traps LW radiation than it reflects SW radiation. Regions of maximum warming below the cloud correspond with optically thicker cloud layers.

Sensitivity Study 1. Many general circulation models (GCMs) specify cloud microphysics using bulk parameters, and some observational retrieval techniques only yield layer-averaged values. Here we examine the impact of these assumptions on an example profile selected from this case at 1615 UTC. Three model runs are performed, one utilizing retrieved profiles of particle size, one utilizing the layer-mean effective radius, and one utilizing a fixed effective radius of 30 μm, which is a common assumption in radiation codes. Figure 2 shows profiles of CRHF for all three-model runs. The solid curve is for the "baseline" case (i.e., using a profile of particle sizes) and shows in-cloud cooling of 1-2 K day^{-1} through the cloud depth.
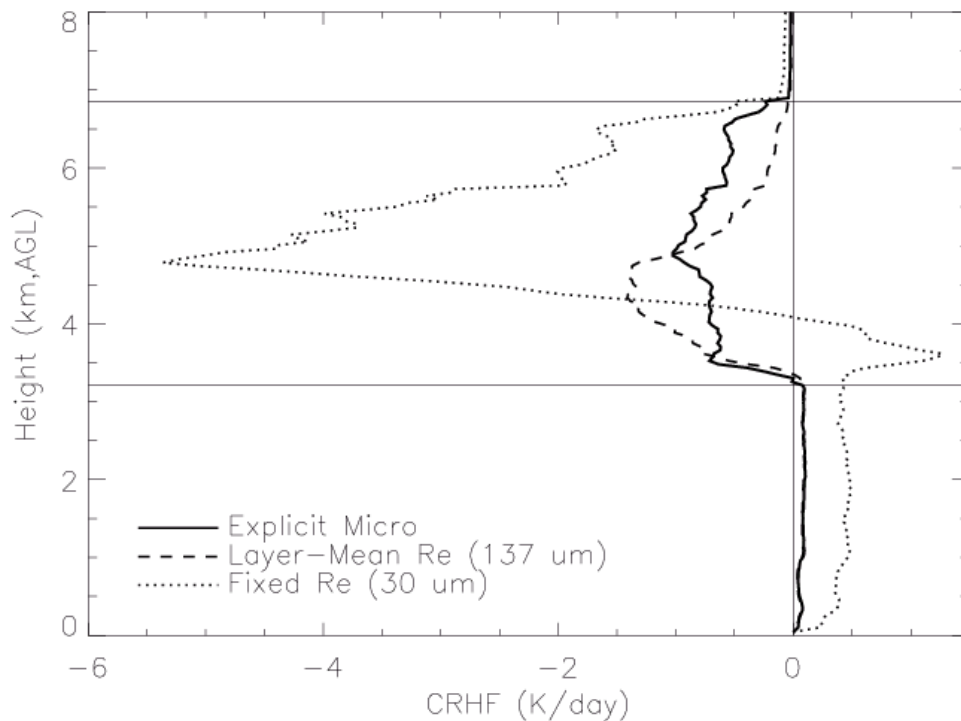
Figure 2. CRHF for various specifications of particle size. Cloud boundaries are designated by horizontal lines.

This cooling is predominantly due to the LW component while the SW component warms but is only about 20% of the LW effect. The dashed curve utilizes an IWC-weighted, layer-averaged retrieved particle size derived from the baseline particle size profile. The average magnitude of the dashed curve is similar to the baseline curve; however, the profile shapes are quite different. While neither cloud is being radiatively destabilized, the cloud modeled using the vertically resolved profile has less of a heating rate gradient throughout the cloud depth than the cloud modeled using the layer-mean effective radius. The impact these two different profiles have on cloud processes is unknown at this time. When the bulk particle size of 30 μm is used, the CRHF profile significantly changes (dotted curve) such that the top portion of the cloud layer cools at a much higher rate and there is a layer of heating near the cloud base. Additionally, with respect to the baseline case, this cloud layer warms the atmosphere below the cloud to a greater degree. The 30-μm particle size assumption results in a cloud optical depth that is roughly quadruple that of the baseline case.

Sensitivity Study 2. Retrievals of cloud IWC and IWP have an uncertainty of about a factor of two. We vary the total IWP of the baseline profile from one tenth to three times the actual retrieved value while the particle size profile is unchanged. The resulting effect on radiative heating rate forcing is shown in Figure 3. As the cloud IWP increases, both the net in-cloud cooling and the below cloud heating rates increase with respect to clear skies. These net changes are primarily due to LW effects, despite opposing SW effects. The net in-cloud heating gradient steepens as the IWP increases due to a net decrease in cooling in the lowest quarter of the cloud depth and increased cooling at the upper part
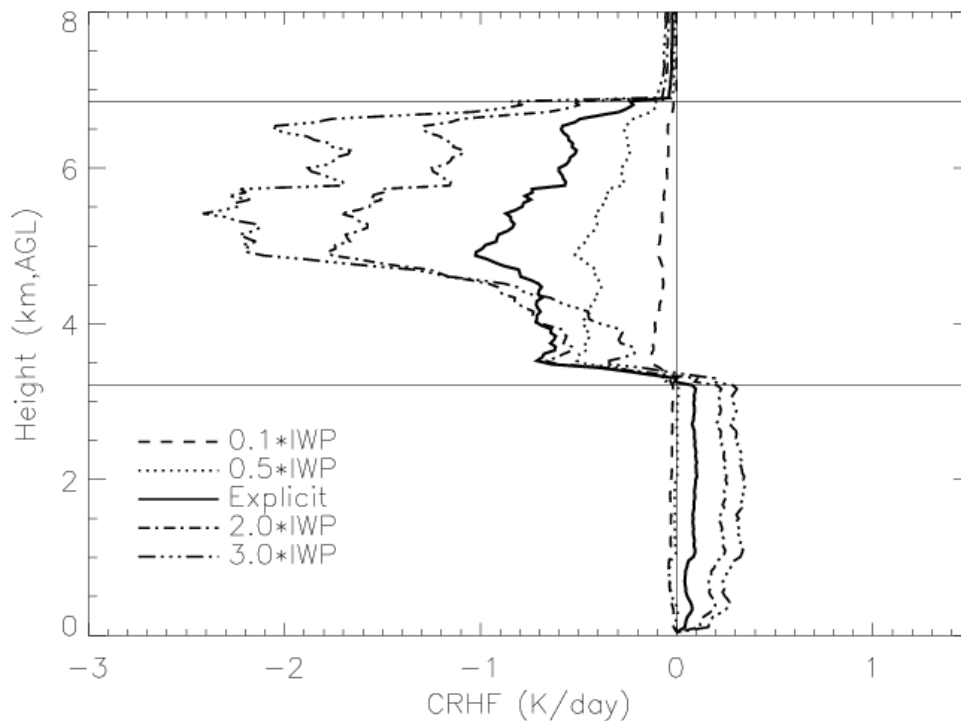
Figure 3. CRHF for various specifications of IWP.

of the cloud. While the variability of heating rates is not linearly related to the uncertainty in cloud microphysical parameters, we see that varying the IWP by a factor of two leads to a similar factor-of-two difference in CRHF at 5 km in our example cloud.

Sensitivity Study 3. By varying the SZA in the heating rate calculation we can approximate the effects of moving this SHEBA cloud case to other Arctic locations (such as the ARM NSA site). The dotted curve in Figure 4 is calculated for SZA=90° (sun at the horizon) and therefore contains no SW contributions. Because LW cooling is not directly affected by SZA, changes in net CRHF profiles are primarily due to SW effects. For the baseline run the SZA was 78.7° (solid curve) and the shape of the CRHF profile is similar to the SZA=90° run. As SZA further decreases, the in-cloud SW heating effect increases with respect to the LW cooling effect, demonstrating the largest impact in the lower portion of the cloud layer. For a SZA of 60° the cloud layer contains regions of both cooling and warming with respect to clear skies. This simple example demonstrates that the impact of Arctic clouds on radiation is not only due to cloud microphysics but also to location and time of year represented by the sun angle.

Mixed-Phase Case - May 4, 1998

Lastly, we examine implications of mixed-phase clouds in radiative transfer calculations using an example profile from May 4, 1998, at SHEBA. Mixed-phase cloud water contents and particle sizes are particularly difficult to specify using surface-based remote sensing techniques. The radar reflectivity
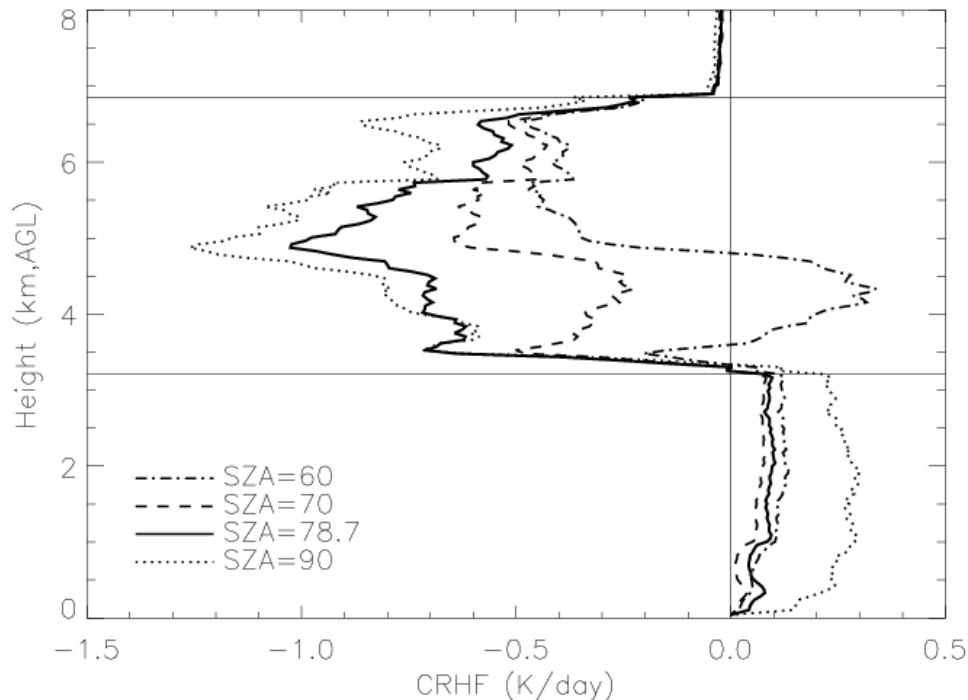
Figure 4. CRHF dependence on SZA.

dependence on the sixth moment of the particle size leads to the larger ice particles dominating the radar reflectivity, while the SW and LW radiation are dominated by the smaller-sized liquid water drops.

Nevertheless, the ubiquity of mixed-phase clouds in the Arctic makes it imperative to consider how best to specify their microphysical properties, to consider what their radiative impacts may be, and to understand how uncertainties in their specification affect heating rate calculations.

The greatest challenge with specifying the vertical profile of mixed-phase cloud microphysics is that, typically, the vertical distribution of the cloud liquid water is unknown. Generally, only the total liquid water path (LWP) is available, often with a large uncertainty. On May 4, a research aircraft flight occurred above the ice camp at SHEBA and sampled a boundary layer, mixed-phase cloud. The aircraft measurements showed that the liquid portion of the cloud extended from approximately 600 to 1100 m in a semi-adiabatic profile. Radar reflectivities suggest the presence of ice particles above, within, and below this liquid layer but are unable to discern the liquid layer base. For the baseline specification of microphysics in this cloud, radar retrievals are used for the cloud ice component and a profile of aircraft measurements are used for the cloud liquid component. To compare with this baseline specification, the liquid parameters are then specified in two separate ways that might be considered if no aircraft data were available.

The solid curve in Figure 5 shows CRHF calculations using the baseline conditions. The dotted curve demonstrates the impact on CRHF if the cloud liquid is distributed semi-adiabatically through the cloud layer (i.e., from near the surface to 1100 m) with the total LWP derived from ground-based microwave radiometer measurements. Such a specification might be reasonable without aircraft or depolarization
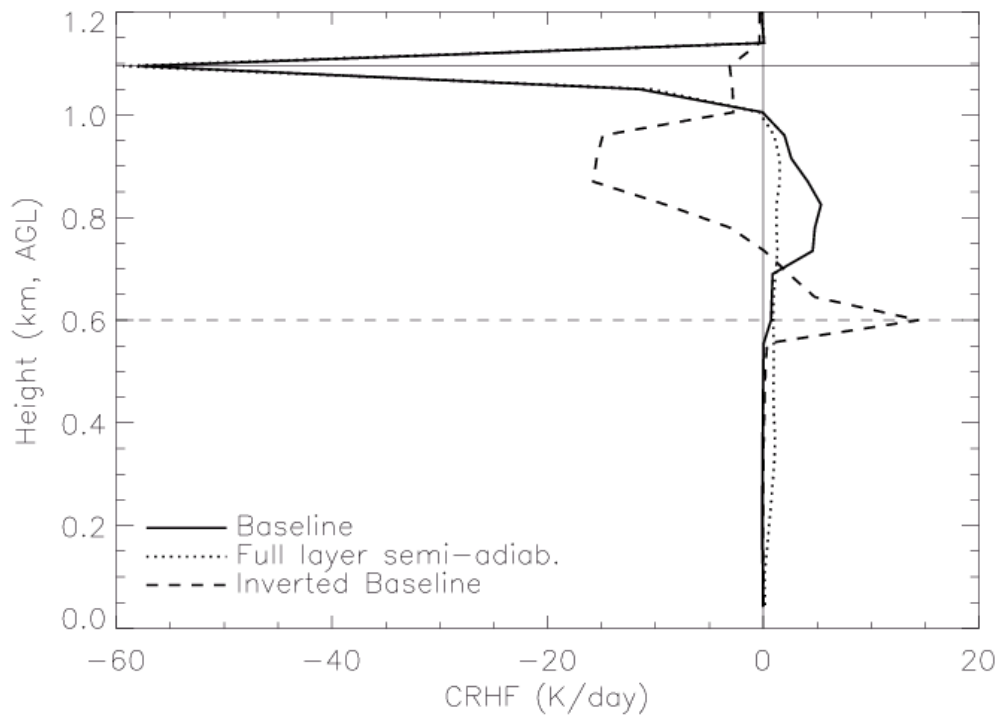
Figure 5. CRHF for different specifications of the liquid phase of a mixed-phase cloud. The liquid layer boundaries, determined from aircraft measurements, are shown as horizontal lines.

lidar measurements for discriminating the location of the liquid phase. The total LW cooling at cloud top is not impacted much by this change in liquid profile; however, there is less warming at lower levels in the cloud. Lastly, to emphasize the importance of how liquid water is distributed in the cloud, CRHF is calculated using the vertically inverting aircraft microphysical profile (dashed curve). Although not necessarily a realistic profile of liquid parameters, this specification is still consistent with ground-based measurements and results in a significant change in the heating rate profile.

Summary

These examples demonstrate some of the implications of calculating atmospheric radiative heating rates with observed profiles of cloud microphysics. Results are shown in terms of profiles of cloud radiative heating rate forcing, or the explicit impact that clouds have on heating rates with respect to clear skies. We have shown that using profiles of ice particle sizes, instead of layer-averaged or fixed particles sizes, significantly modifies heating rate profiles. Furthermore, the uncertainty in cloud IWP, and its specification in the radiative transfer model, has an impact both on the average heating rates and on the vertical gradient of heating within a cloud/atmosphere layer. By varying the SZA in one model run, we have also demonstrated that location with respect to the sun plays a critical role in the manner in which clouds interact with radiation. Finally, we have explored some of the implications of mixed-phase cloud specification in heating rate calculations, in particular the vertical distribution of liquid phase in the

cloud. This preliminary study has indicated that, without instrumentation to discriminate cloud phase, large and potentially inaccurate assumptions about mixed-phase cloud structure will have to be utilized for heating rate calculations.

Presented here is a sample of the potential uses of vertically resolved cloud microphysics data with a radiative transfer code. Many months of cloud microphysical properties from both SHEBA and the ARM NSA site are now available and are displayed on the Internet at: www.etl.noaa.gov/arctic. In future studies with these tools we will assess the sensitivity of heating rate calculations to the input parameters, including the cloud microphysics and other surface and atmospheric properties. We will thus be able to better understand the potential impacts of uncertainties in these parameters. Furthermore, studies using these tools can clarify the impact of various GCM cloud property assumptions and provide insight into potential improvements to these assumptions.

Acknowledgments

Corresponding Author

M. D. Shupe, matthew.shupe@noaa.gov, (303) 497-6471

References

Chen, B., D. H. Bromwhich, K. M. Hines, and X. Pan, 1995: Simulations of the 1979-1988 polar climates by global climate models. *Ann. Glaciol.*, **21**, 85-90.

Key, J., 2001: "Cooperative Institute for Meteorological Satellite Studies." *Streamer User's Guide*, p. 96, University of Wisconsin.

Key, J., P. Yang, B. Baum, and S. Nasiri, 2002: Parameterization of shortwave ice cloud optical properties for various particle habits. *J. Geophys. Res.*, in press.

Matrosov, 1999: Retrievals of vertical profiles of ice cloud microphysics from radar and IR measurements using tuned regressions between reflectivity and cloud parameters. *J. Geophys. Res.,* **104**, 16,741-16,753.

Ramanathan, V., R. D. Cess, E. F. Harrison, P. Minnis, B. R. Barkstrom, E. Ahmad, and D. Hartman, 1989: Cloud-radiative forcing and climate: Results for the Earth Radiation Budget Experiment. *Science*, **243**, 57-63.

Shupe, M. D., T. Uttal, S. Y. Matrosov, and A. S. Frisch, 2001: Cloud water contents and hydrometeor sizes during the FIRE Arctic Clouds Experiment. *J. Geophys. Res*., **106**, 15,015-15,028.

Tao, X., J. E. Walsh, and W. L. Chapman, 1996: An assessment of global climate model simulations of Arctic air temperatures. *J. Climate*, **9**, 1060-1076.

Uttal, T., et al., 2002: Surface Heat Budget of the Arctic Ocean. *Bull. Am. Met. Soc*., **83**, 255-275.